# Roles of Dislocations and Grain Boundaries in Martensite Nucleation

S. KAJIWARA

In order to elucidate roles of dislocations and grain boundaries in martensite nucleation, the transformation temperature $(M_s)$ of specimens austenitized at various temperatures and subjected to prestrain has been measured, using Fe-Ni, Fe-Ni-C, and Fe-Cr-C alloys. It is concluded that the plastic accommodation, in austenite, of the shape strain of the transforming martensite is a vital step in the nucleation event. Any factors impeding such plastic accommodation, such as the lack of dislocations, work hardening, and grain refinement, suppress the transformation. Contrary to the general belief, dislocations themselves do not act as favorable nucleation sites. Grain boundaries provide nucleation site, but only certain types of grain boundaries are qualified to be potential nuclei. A quantitative analysis shows that the increasing difficulty for the plastic accommodation with decreasing grain size is the main factor to depress $M_s$ in fine-grained specimens.

## I. INTRODUCTION

ONE of the classical problems in the martensitic transformation is what kind of lattice defects could be the most favorable nucleation site. It is generally believed that dislocations and grain boundaries are favorable nucleation sites. However, in the literature there is no systematic work to confirm this proposition, although this problem has been repeatedly discussed by many investigators.[1-8] The primary aim in the present work is to clarify the role of dislocations and grain boundaries in the martensite nucleation. For this purpose, experiments were designed to separate the effect of the existence of dislocations on the martensitic transformation temperature $(M_s)$ from the other effects.

Another part of this work concerns the effect of grain size on the $M_s$ temperature which is closely related to the above basic problem. This has been originally treated as one of the effects of different austenitizing conditions,[9-15] but it is now established that the variation of $M_s$ with austenitizing condition is mainly due to the difference in grain size.[16] The most plausible explanation for the grain size effect seems to be that of Ansell and his co-workers.[17,18] They proposed that the increased strength of austenite by grain refining makes it more difficult to accommodate plastically the shape strain of the transforming martensite plate, thus depressing the $M_s$ temperature in fine-grained specimens. This proposal is a logical extension of their theory[19-22] that the strengthening of austenite, whatever may cause it, increases substantially non-chemical free energy opposing the transformation. Although they showed some experimental evidence for their proposition,[17,18,22] their analysis is rather qualitative, and moreover most of their work was done on alloys with $M_s$ higher than room temperature, which inevitably involves some effect of diffusion. In the present work, a quantitative analysis is given to the results obtained with alloys having $M_s$ lower than room temperature.

## II. EXPERIMENTAL

Fe-Ni, Fe-Ni-C, and Fe-Cr-C alloys of which the chemical composition is shown in Table I were used in the experi-

**Table I. Chemical Composition of Alloys (Wt Pct)**

| No. | Alloy | Ni | Cr | C | Fe |
|-----|-------------|-------|------|------|------|
| 1 | Fe-33.11Ni | 33.11 | — | — | bal. |
| 2 | Fe-33.24Ni | 33.24 | — | — | bal. |
| 3 | Fe-33.75Ni | 33.75 | — | — | bal. |
| 4 | Fe-37.6Ni | 37.59 | — | — | bal. |
| 5 | Fe-31Ni-0.3C | 31.06 | — | 0.29 | bal. |
| 6 | Fe-30Ni-0.4C | 29.99 | — | 0.39 | bal. |
| 7 | Fe-28Ni-0.6C | 28.06 | — | 0.59 | bal. |
| 8 | Fe-34Ni-0.4C | 34.06 | — | 0.40 | bal. |
| 9 | Fe-9Cr-1.1C | — | 8.78 | 1.09 | bal. |
| 10 | Fe-10Cr-1.1C | — | 9.85 | 1.10 | bal. |

ment. The $M_s$ temperatures of these alloys are all below room temperature, and alloys No. 5 to 7 were designed to have approximately the same $M_s$ temperature by adjusting Ni and C contents. The alloys, except Nos. 2 and 3, were prepared by vacuum melting, using "electric" iron, high purity nickel, chromium, and carbon. Ingots of mass 3 kg and dimensions 45 × 64 × 100 mm were forged and hot-rolled to 20 mm thickness. After removing the surface scale, specimens of dimensions 15 × 15 × 70 mm were homogenized in evacuated silica capsules at 1370 K for one week for alloys No. 1, 4 to 8 and at 1540 K for 48 hours for alloys No. 9 and 10. Alloys No. 2 and 3 were made by arc-melting in argon, in which decarburized iron plates (less than 20 ppm C) prepared from "electric" iron and high purity nickel (99.99 pct) were used as starting materials. The arc-melted specimens were homogenized at 1370 K for one week. In order to remove impurity atoms such as C and O, specimens of Fe-Ni alloys (Nos. 1 to 3) with 1.5 mm thickness were heated at 1670 K for 5 hours in purified dry hydrogen. Specimens of all the alloys were finally cold-rolled to thickness of 0.5 mm, from which strips of 3 × 20 mm and mechanical test pieces with the gauge length of 15 mm were cut out. These specimens were austenitized at various temperatures to obtain different grain sizes (Table II). Fe-Ni alloys were annealed at each temperature for 3 hours in purified dry hydrogen and then furnace-cooled to room temperature, while Fe-Ni-C and Fe-Cr-C alloys were heated for 1 hour in evacuated silica capsules and quenched in brine by breaking the capsules. The specimen thickness of the latter alloys containing car-

S. KAJIWARA is Laboratory Head, National Research Institute for Metals, 2-3-12 Nakameguro, Meguro-ku, Tokyo 153, Japan.

**Table II. Grain Sizes of Specimens Austenitized at Various Temperatures (Unit: $\mu$m)**

| Alloy | Austenitizing Temperature (K) | | | | | | |
|---|---|---|---|---|---|---|---|
| | 970 | 1070 | 1120 | 1170 | 1370 | 1470 | 1670 |
| Fe-33.11Ni | 20 | 25 | — | 75 | 290 | — | 630 |
| Fe-33.24Ni | 10 | — | — | 55 | 200 | — | 670 to 800 |
| Fe-33.75Ni | 10 | — | — | 55 | 190 | — | 660 to 800 |
| Fe-31Ni-0.3C | 20 | — | 40 | 60 | 210 | 215 | — |
| Fe-30Ni-0.4C | 20 | 25 | 40 | 75 | 205 | 275 | — |
| Fe-28Ni-0.6C | — | 25 | 35 | 90 | 220 | 280 | — |

bon was then reduced from 0.5 mm to 0.4 mm by chemical polishing in order to remove the surface layer which may have been decarburized during the heat treatment in vacuum. The specimens thus austenitized were used for the measurement of electrical resistance change with temperature to determine the $M_s$ temperature. The resistance measurement was performed by the four point method using a constant current of 0.4 to 0.8 A, where the connection of copper leads and a thermocouple to the specimens was made by solder with a low melting point (343 K), not by the spot welding, to avoid plastic deformation. In this measurement the specimens were cooled in a simple way: a copper block containing a cavity where a specimen is placed was slowly lowered into a deep Dewar half filled with liquid nitrogen. The measurements of $M_s$ temperatures for small specimens (2 × 3 × 0.5 mm) were made by cooling stepwise at the interval of 10 K, and examining, at each step, the specimen surface metallographically at room temperature. The specimens with $M_s$ below 77 K were directly immersed in liquid helium. The purpose of the experiment with small specimens will be described later.

The prestrain was introduced in austenite at room temperature either by extension, indentation, or rolling. The yield stress of austenite was measured by an Instron type machine with a strain rate of 2 × $10^{-4}$/sec at temperatures between 77 K and 300 K. Low temperature tests were conducted in properly cooled isopentane and in liquid nitrogen.

## III. RESULTS AND DISCUSSION

### A. Effect of Prestrain on $M_s$ Temperature

Figures 1 through 3 show $M_s$ temperatures of as-annealed and prestrained specimens (extended by 1 pct) for various grain sizes in Fe-Ni alloys. It is noted that the $M_s$ temperature of as-annealed specimens with large grain sizes, which were austenitized at 1370 K and 1670 K, is very much scattered. The range of the scatter is, for example, from below 77 K to 200 K for 630 $\mu$m grain of Fe-33.11Ni (Figure 1) and from below 4 K to 130 K for 800 $\mu$m grain of Fe-33.75Ni (Figure 3). On the other hand, the $M_s$ temperatures of prestrained specimens are confined to a rela-
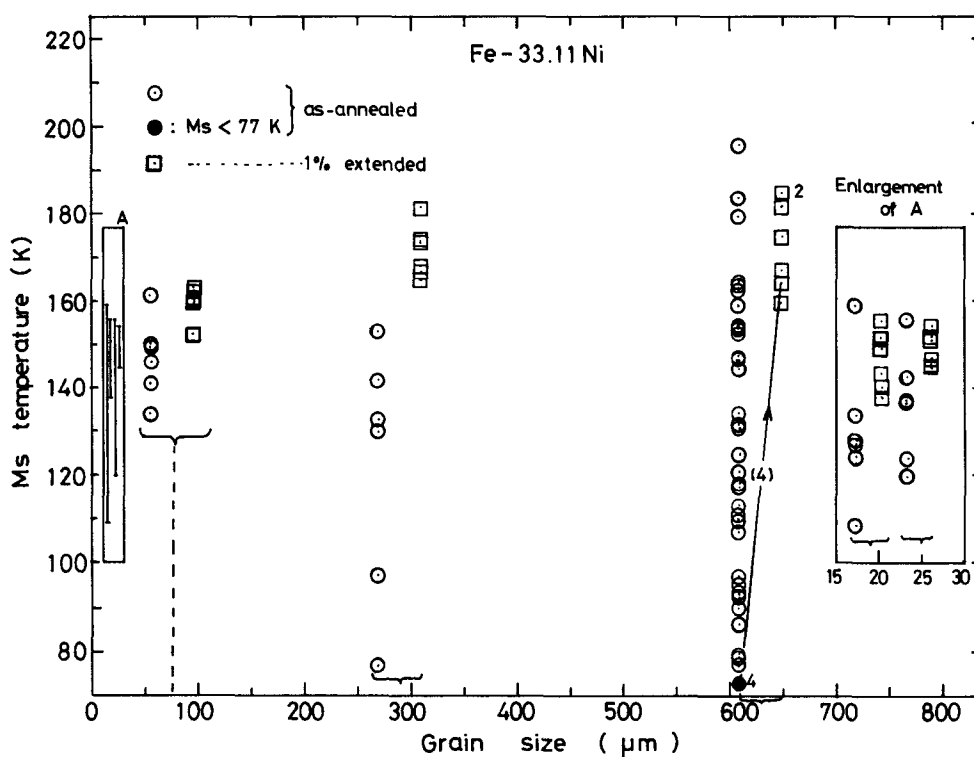


Fig. 1—$M_s$ temperatures of Fe-33.11Ni for various grain sizes. Circles and squares represent $M_s$ for as-annealed and 1 pct extended specimens, respectively. For small grain sizes a figure with an enlarged abscissa is inserted in the right. Arrow indicates an increase in $M_s$ temperature caused by 1 pct extension. Numeral at the symbol shows the number of specimens which have the same $M_s$ temperature. Numeral in parentheses indicates the number of specimens of which the $M_s$ temperatures were raised by 1 pct extension from below 77 K or 4 K.
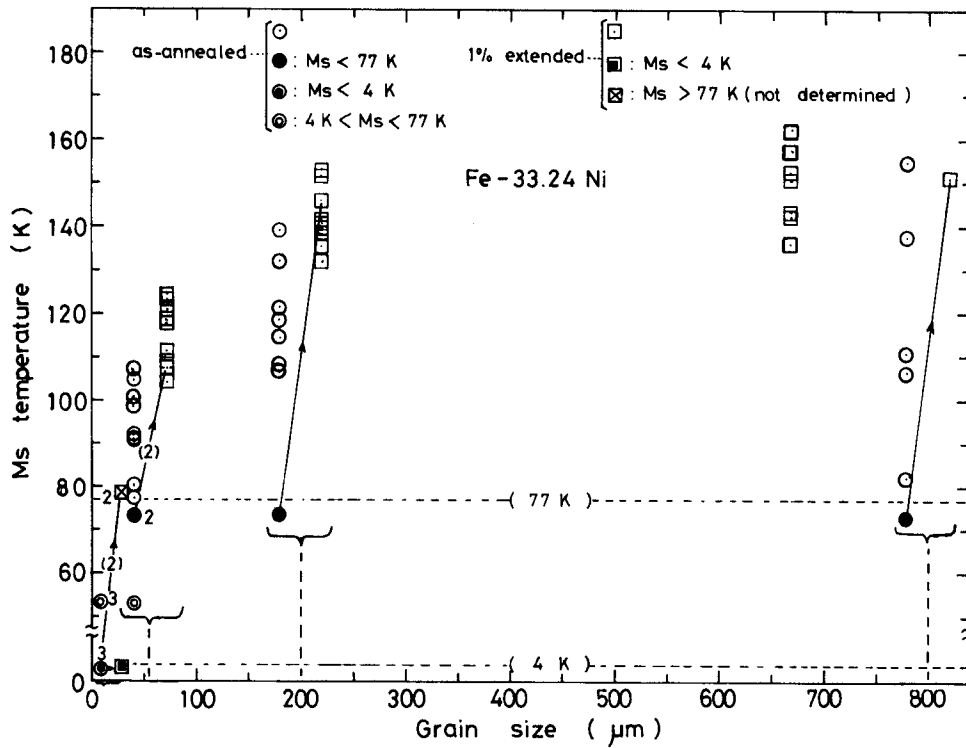
Fig. 2—$M_s$ temperatures of Fe-33.24Ni for various grain sizes. The same notation as in Fig. 1 is used. Although the alloy composition is scarcely different from that of Fig. 1, $M_s$ for small grain size is greatly decreased.
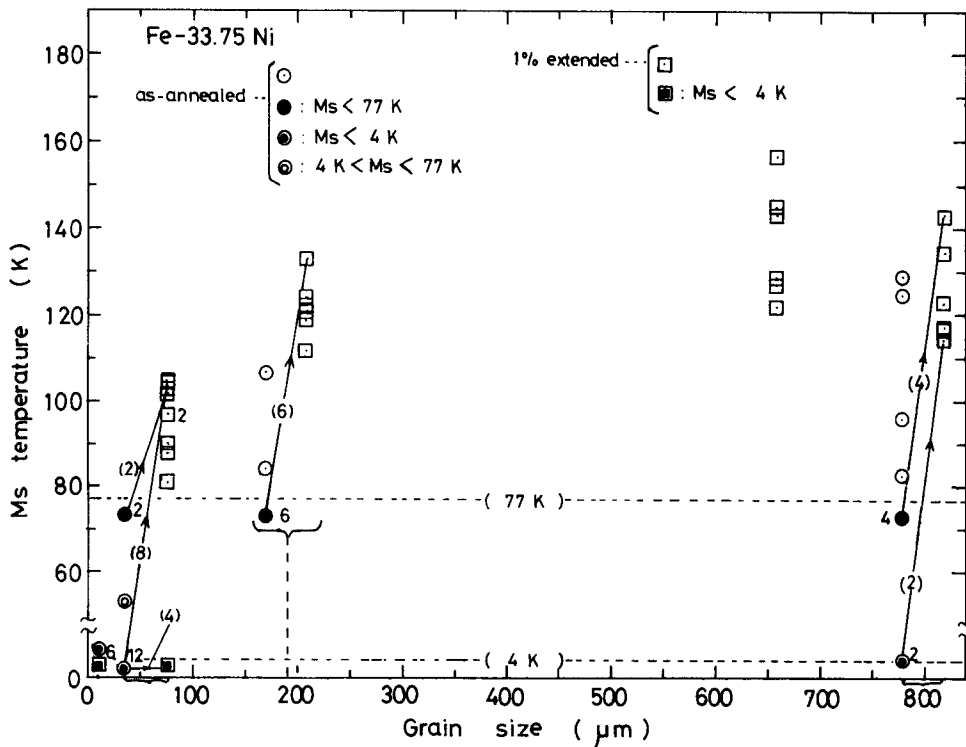


Fig. 3—$M_s$ temperatures of Fe-33.75Ni for various grain sizes. The same notation as in Fig. 1 is used. Note that the $M_s$ temperatures for 10 $\mu$m grain are all below 4 K.

tively narrow range of about 30 K even for these large grains and they are generally higher than those for the as-annealed specimens. In order to know more explicitly the effect of prestrain on $M_s$, those annealed specimens which had not been transformed even when cooled down to 77 K

or 4 K at the first test were subjected to extension by 1 pct at room temperature and then cooled again for the measurement of $M_s$ temperature. The $M_s$ temperatures at the second test were raised very much as indicated by arrows in Figures 1 through 3; in some cases the rise in $M_s$ amounts

to more than 100 K. For small grain size specimens, however, the prestraining was not so effective in raising $M_s$; for example, the $M_s$ temperatures for 10 $\mu$m grain size in Fe-33.75Ni were all below 4 K for both the annealed and the prestrained states (Figure 3). The first important question to be answered in the present work is what factor is responsible for such a large increase in $M_s$ temperature on prestraining in the case of large grain size.

The 1 pct extension, of course, introduces dislocations in the specimen. Two hypotheses can be considered about the role of these dislocations in raising the $M_s$ temperature. One is that the dislocations themselves provide favorable nucleation sites for the martensitic transformation (hypothesis 1). The other is that these dislocations merely serve to initiate slip in austenite for the plastic accommodation of the nucleating martensite plate (hypothesis 2). Unless prestrained, the plastic accommodation would be difficult in most of the specimens annealed at very high temperatures, such as 1370 K and 1670 K, because of the lack of dislocations. In the latter hypothesis it is assumed that favorable nucleation sites exist at grain boundaries and, for the martensite nucleation, dislocations must exist around the nucleation sites to initiate slip.

To test these hypotheses, the following experiment was carried out. Strips (3 × 20 × 0.5 mm) of Fe-33.11Ni with very large grains, annealed at 1670 K, were first extended by 1 pct at room temperature and then cut into pieces with 2 mm width by a multi-wire saw. The cut edges were electrolytically polished to remove deformed regions introduced by the cutting. The $M_s$ temperatures of such small specimens (2 × 3 × 0.5 mm) were measured and the results are shown against the number of grains per specimen in Figure 4. Each of the original strips from which the small specimens were cut out is denoted by A, B, C, D, or E in Figure 4. The hatching in the upper right corner of this figure shows the range of the $M_s$ temperature of large specimens (3 × 20 × 0.5 mm) extended by 1 pct. If hypothesis 1 is correct, the $M_s$ temperatures of these small specimens will be the same as those for large specimens because each specimen still contains dislocations which



Fig. 4—$M_s$ temperatures of small specimens (2 × 3 × 0.5 mm) prestrained by 1 pct. The number of grains per specimen is shown in the abscissa. Those specimens with the same symbol were taken from an identical original specimen.

were introduced by 1 pct extension* before the cutting. If

hypothesis 2 is correct, the $M_s$ temperature will be lowered because the number of grains per specimen is reduced more than by an order of magnitude by the cutting. Such a reduction in the number of grains will seriously affect the $M_s$ temperature when the total number of grains becomes very small as in the present case, for hypothesis 2 assumes that grain boundaries provide nucleation sites. The results shown in Figure 4 support hypothesis 2. In comparison with large specimens, the $M_s$ temperature is much lowered for most of these small specimens; especially, the $M_s$ temperature of one of the single crystalline specimens is below 77 K. Near the dotted line in the upper part of Figure 4, there are seen several specimens which have $M_s$ temperatures comparable to those of large specimens. The existence of the specimen with such a high $M_s$ temperature is explained, according to hypothesis 2, in that the specimen happened to contain grain boundaries which act as favorable nucleation sites. Each of the original large specimens, except specimen A, had contained such a piece (see the symbol in Figure 4). Owing to this, the $M_s$ temperatures of the original large specimens would fall in the range shown by the hatching in Figure 4, if they were measured before the cutting.

One may argue the above experimental facts in another way in that all the differences in $M_s$ temperature shown in Figure 4 result from microscopic inhomogeneities in the dislocation structure produced by 1 pct extension; that is, clustered or tangled dislocations provide a favorable nucleation site. However, this sort of the reasoning is negated by the following experiment.

Small specimens of 2 × 3 × 0.5 mm cut from strips of Fe-33.11Ni which had been annealed at 1670 K for 4 hours were first cooled to 77 K, and those specimens which had not been transformed above 77 K were selected for the second cooling. Before cooling again, one micro-Vickers indent of 200 g was made "within" a grain of each specimen at room temperature. Such indentation will produce a high density of dislocations which are localized in a small region. The results of the measurement of $M_s$ for these indented specimens are shown in Figure 5. The $M_s$ temperatures of the specimens were not raised very much by the indentation except a few cases (ones at the upper right corner in the figure). For the specimens marked by downward arrows, no martensitic transformation occurred at the second cooling down to 77 K. These specimens were cooled for the third time after making another indent "right on" a grain boundary. The indentation on a grain boundary will produce a more complicated dislocation structure than in the case of the indentation within a grain. The results of the third cooling are shown by filled circles. One of these specimens, marked with double arrow in Figure 5, was not transformed again down to 77 K. Before cooling this specimen for the fourth time, the indentation was made on all the grain boundaries (one indent at each boundary), the total number of indents being as many as thirty. It turned out that such indentation could not bring either $M_s$ temperature above 77 K. This specimen was transformed finally by immersing in liquid helium. These facts clearly indicate that a highly localized, complicated distribution of dislocations does not
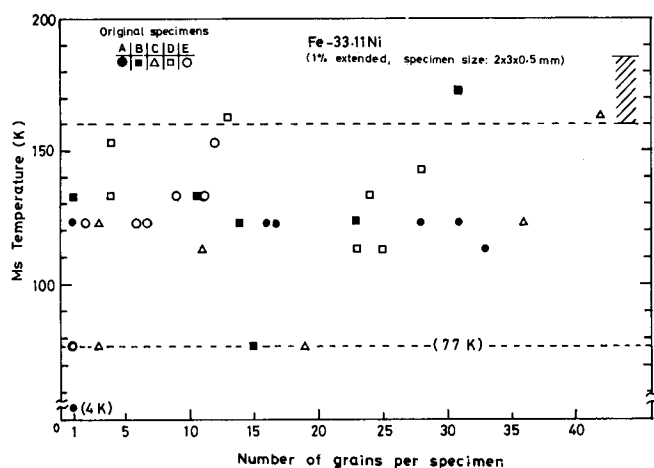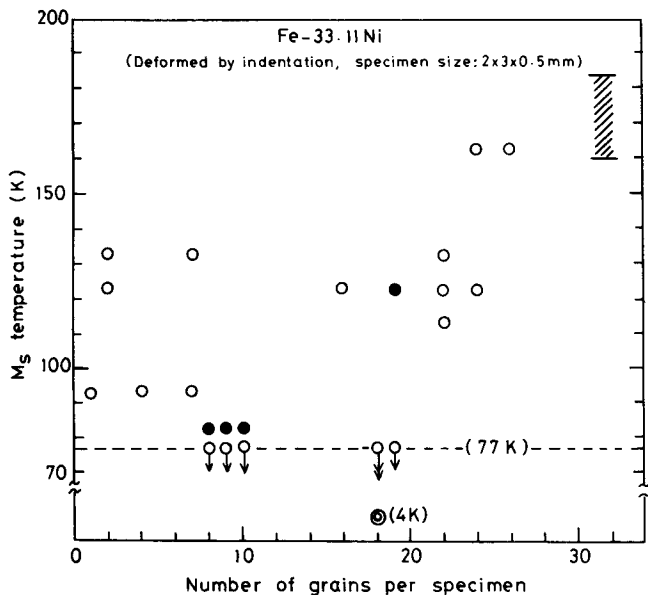
Fig. 5—$M_s$ temperatures of small specimens deformed by indentation. All the specimens had $M_s$ below 77 K before the indentation. Open, filled, and double circles denote $M_s$ for the 2nd, 3rd, and 4th cooling, respectively. Specimens were indented each time before the cooling.

provide a favorable nucleation site either, thus denying hypothesis 1.

According to hypothesis 2, grain boundaries are supposed to act as nucleation sites. However, from the following facts, we presume that all the grain boundaries can not be favorable nucleation sites. First, in Figure 4 there are two specimens containing grains as many as 15 and 20, of which the $M_s$ temperatures are very low. Second, in the experiment just mentioned above, the $M_s$ temperature of the specimen which was indented at every grain boundary was still below 77 K. For both cases, if the specimen contained a grain boundary suitable for the nucleation site, it would be transformed at the normal $M_s$ temperature because dislocations necessary to initiate the accommodation slip are also available around the nucleation site. The probability of finding a grain boundary suitable for the nucleation site may be about 1/500, judging from the fact that prestrained specimens of 3 × 20 × 0.5 mm with 600 to 800 $\mu$m grain size, each of which contains about 500 grain boundaries in average,*

---

*In the estimation of the number of grains per specimen, the fact that the grains in these specimens had a bamboo type structure was taken into account, and the shape of a grain was assumed to be hexagonal.

---

were all transformed in the normal $M_s$ temperature range (Figures 1 through 3). Thus we can conclude that a boundary suitable for the nucleation site must have some special character, although we could not identify the exact nature of such boundary.

The ineffectiveness of prestrain in raising $M_s$ for small grain size can be explained in that a sufficient number of dislocations for the initiation of the accommodation slip already exist in the as-annealed state because of low austenitizing temperature. The same reasoning is given to an experimental fact that the $M_s$ temperature of as-annealed specimens with small grain sizes is not very much scattered (Figures 1 through 3).

## B. Effect of Grain Size on $M_s$ Temperature

Average values of the $M_s$ temperatures for the specimens shown in Figures 1 through 3 are replotted in Figure 6 to see the grain size effect more clearly. For the as-annealed specimens with large grain size, no meaningful averages of $M_s$ could be taken because of the large scatter. The $M_s$ temperature decreases with decreasing grain size as reported in many previous papers.[10-19] It is noted that this decrease in $M_s$ is greater for higher Ni contents; the $M_s$ decreases from 120 K for 190 $\mu$m grain to below 4 K for 10 $\mu$m grain in Fe-33.75Ni, while it decreases from 170 K for 290 $\mu$m grain to 145 K for 20 $\mu$m grain in Fe-33.11Ni. Since the difference in Ni content between these alloys is small, such behavior is not attributed to the Ni content itself. It seems to be related to the height of the plateau level in the $M_s$ vs grain size curve; that is, the depression of $M_s$ by grain refining becomes more prominent with decreasing plateau level. A similar trend was also observed on Fe-Ni-0.4C alloys with various Ni contents (Ni: 26 to 30 pct). Hereafter this plateau temperature on the $M_s$ vs grain size curve is denoted as $T_p$. Figure 7 shows the grain size effect on $M_s$ for Fe-Ni-C alloys (Nos. 5 through 7) with about the same $T_p$ as that of Fe-33.75Ni. All of the three curves in this figure are similar to that of Fe-33.75Ni, so we can say that the C content does not influence the dependence of $M_s$ on grain size if $T_p$ is kept constant by adjusting the composition of other elements of the alloy. Here we note that the martensite formed in these Fe-Ni-C alloys (Nos. 5 through 7) is all plate-like for any grain size, while the martensite in Fe-33.75Ni is lenticular. This means that the martensite morphology does not influence the shape of the $M_s$ vs grain size curve, either. Possible reasons for the influence of $T_p$ on the curve shape will be discussed later.

It is noted in Figure 7 that the scatter in $M_s$ in Fe-Ni-C alloys is not so large even for large grain size. This is probably because the austenitized specimens were quenched in brine, which will cause some degree of deformation. The "as-quenched" specimens of Fe-Ni-C alloys are then equiva-
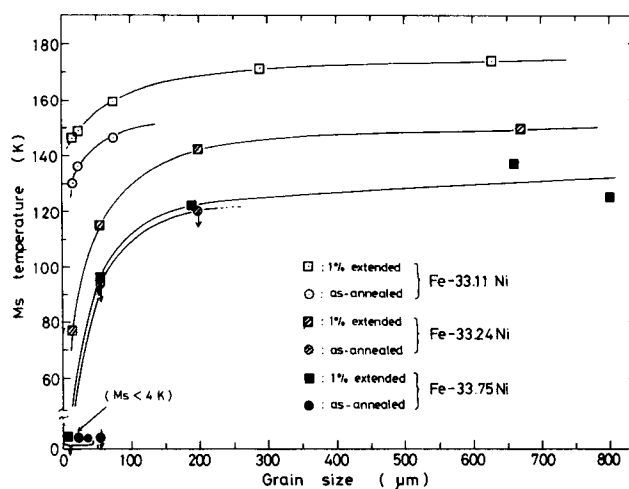


Fig. 6—Effect of grain size on $M_s$ temperature in Fe-Ni alloys. Average values of the $M_s$ temperatures shown in Figs. 1 through 3 are replotted. The values for large grains of annealed specimens were excluded because of the extremely large scatter in $M_s$. Downward arrows indicate that there exist a few specimens with $M_s$ below 77 K or 4 K besides those averaged.
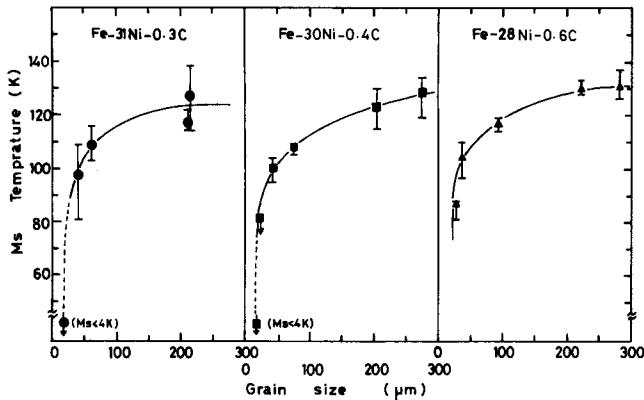
Fig. 7—Effect of grain size on $M_s$ temperature in Fe-Ni-C alloys with the same "$T_p$" temperature. Each point represents the average value of $M_s$ for five measurements.

lent to prestrained specimens of Fe-Ni alloys which were furnace-cooled from the austenitizing temperatures.

We now discuss the factors suppressing martensitic transformation in fine-grained specimens. As was emphasized in the preceding section, the plastic accommodation of the shape strain of the transforming martensite plate is an important necessary condition for the martensite nucleation. In the case of polycrystals, such plastic accommodation will be increasingly difficult with decreasing grain size because of the following reason. The deformation by slip to accommodate the martensite shape strain can not be confined to one grain, but it must be propagated into neighboring grains. A critical stress to cause such slip propagation corresponds to yield stress in polycrystals which is increased with decreasing grain size. The increased difficulty in the plastic accommodation of the martensite shape strain is the only conceivable reason for the suppression of the transformation in fine-grained specimens, because the other necessary conditions for the martensite nucleation described in the preceding section are satisfied in these specimens; that is, there exist a sufficient number of dislocations to initiate slip, as well as grain boundaries which can act as favorable nucleation sites. To prove this proposition, a quantitative analysis was made on alloys No. 1 through 3 and 5 through 7.

As is well known, the shape strain accompanying the martensitic transformation is divided into two components; one is a shear strain ($\gamma$) along the habit plane, the other is a dilatational strain ($\varepsilon$) normal to the habit plane which corresponds to the volume expansion.[23] The energy, $W$, expended in deforming the austenite in order to accommodate the shear strain is $\gamma\tau$ per unit volume of martensite, where $\tau$ is a resistive shear stress acting on the martensite. If the shear direction and shear plane ($i.e.$, the habit plane) of the martensite shape strain coincide with those of the slip system in austenite, $\tau$ should be equal to a critical shear stress, $\tau_c$, for the propagation of slip into a neighboring grain. However, since it is not the case, $\tau$ is related to $\tau_c$ by $m\tau = \tau_c$ where $m$ is an orientation factor analogous to the Schmid factor and can be derived after Hirth and Loth.[24] $\tau$ is further related to the tensile yield stress, $\sigma$, of polycrystals, using the relation $\sigma = M\tau_c$ where $M$ is the Taylor orientation factor.[25,26,27] Thus we have

$$W = \gamma\sigma/mM = \alpha\sigma \qquad [1]$$

where $\alpha = \gamma/mM$. The deformation energy associated with the dilatational strain $\varepsilon$ can be neglected to the first approximation, because $\varepsilon$ is smaller by an order of the magnitude than $\gamma$; especially in the present case, it is very small (1 to 2 pct) due to the Invar effect of the austenite in the alloys involved.* In Eq. [1], $\sigma$ is increased with decreasing grain

---

*The author observed an abnormally small temperature dependence of the lattice parameter for the present Fe-Ni-C alloys (Nos. 5 through 8). The Invar effect in Fe-Ni alloys with 33 to 37 pct Ni has been well established in the literature.

---

size, $d$; the most well-known relation is the Hall-Petch relation;[28,29] that is,

$$\sigma = \sigma_0 + k/\sqrt{d} \qquad [2]$$

where $\sigma_0$ and $k$ are material constants independent of $d$. Therefore, with decreasing $d$, $W$ is increased and this extra energy must be supplied by chemical driving energy; thus the $M_s$ temperature is lowered. Since $\sigma$ is also increased with decreasing temperature, the overall increase in $W$ is the sum of those due to grain size and temperature, $T$.

In order to test the theory mentioned above, we must know $\sigma$ at the $M_s$ temperature, denoted as $\sigma(M_s)$, for various grain sizes and the corresponding chemical driving energy, and compare the relation between them with that of Eq. [1]. (The values of $\gamma$, $m$, and $M$ in Eq. [1] are known, either experimentally or theoretically.) Since $\sigma(M_s)$ can not be directly measured because the stress-induced martensitic transformation occurs before yielding by slip, we have employed the following procedures. The yield stress of austenite at room temperature, $\sigma(RT)$, was first measured for various grain sizes (Figure 8), and then $\sigma(M_s)$ was estimated from $\sigma(RT)$, assuming that the temperature dependence of $\sigma$ is the same as that of an alloy which has a similar alloy composition but is not transformed by tensile tests at temperatures down to 77 K. Fe-37.6Ni (alloy No. 4) and Fe-34Ni-0.4C (alloy No. 8) have such character and will represent the temperature dependence of $\sigma$ for alloys No. 1 through 3 and alloys No. 5 through 7, respectively. The measured $\sigma$ vs $T$ curves for these nontransforming alloys are shown in Figure 9. The results in Figure 8 indicate that the Hall-Petch relation seems to hold for the present alloys. The
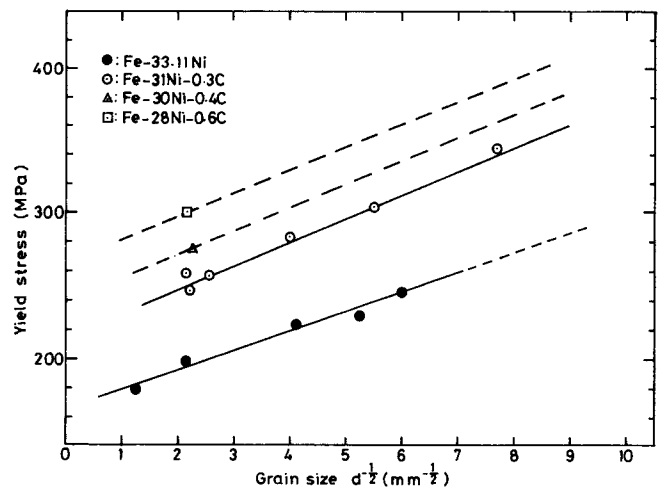


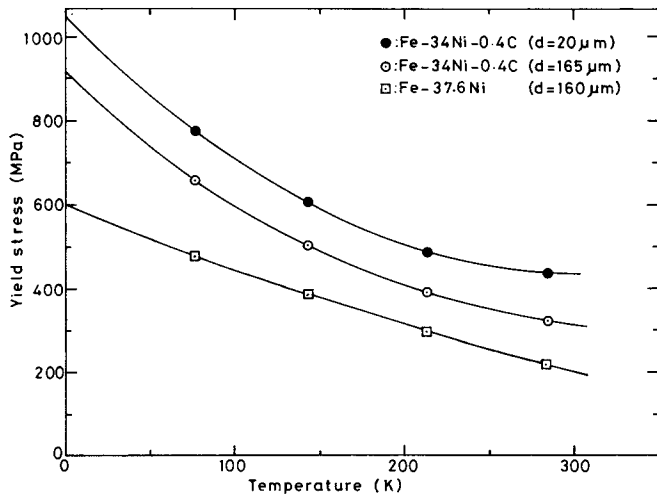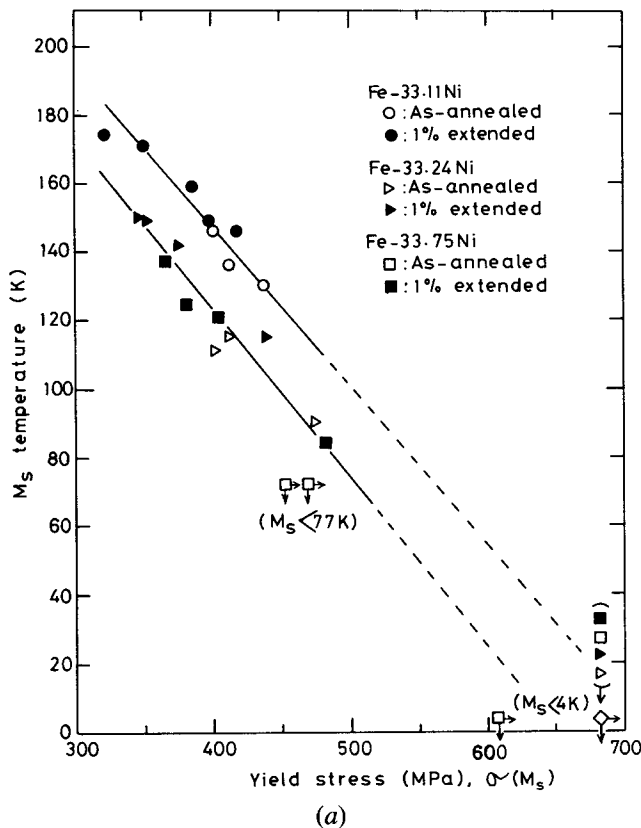Fig. 8—Effect of grain size on yield stress of austenite at room temperature.

Fig. 9—Effect of temperature on yield stress of austenite.

values of $\sigma(RT)$ for Fe-30Ni-0.4C and Fe-28Ni-0.6C were determined from dotted lines in Figure 8 which were drawn through the measured points for large grains, assuming the same slope to that of Fe-31Ni-0.3C. For Fe-33.24Ni and Fe-33.75Ni, the straight line for Fe-33.11Ni in Figure 8 was used to obtain $\sigma(RT)$. As shown in Figure 9, there is no difference in the temperature dependence of $\sigma$ between large and small grain size specimens.

The values of $\sigma(M_s)$ thus obtained from Figures 8 and 9 are plotted in Figures 10(a) and (b) in relation to the corresponding $M_s$ temperatures. The $M_s$ decreases with in-

creasing $\sigma(M_s)$ in an approximately linear fashion. The chemical driving energies, $\Delta G$, corresponding to different $M_s$ temperatures, were obtained by the driving energy vs temperature curves in Figure 11 which were calculated after Kaufman and Cohen[30] for Fe-Ni alloys, and for Fe-Ni-C alloys, with a similar equation based on the regular solution model. Figures 12(a) and (b) show the relation between $\sigma(M_s)$ and $\Delta G$; a linear relationship is obtained although there is a considerable scatter for Fe-Ni alloys. The increase in $\Delta G$ in this figure should correspond to the increase in $W$ due to the increase in $\sigma$ according to Eq. [1]. Therefore the slope in the figure should be equal to the proportional coefficient ($\alpha$) in Eq. [1].
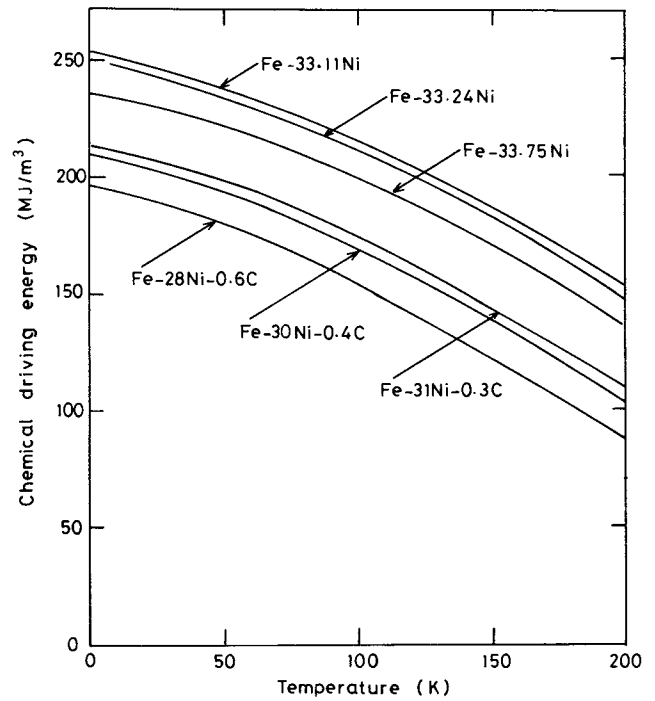


Fig. 11 — Chemical driving energy vs temperature curves calculated by the regular solution model.
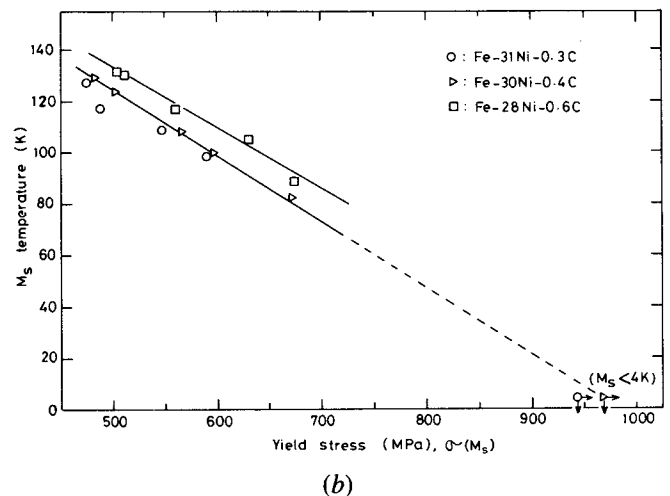


(a)



(b)

Fig. 10—Relation between $M_s$ temperature and yield stress of austenite at $M_s$: (a) for Fe-Ni alloys and (b) for Fe-Ni-C alloys.
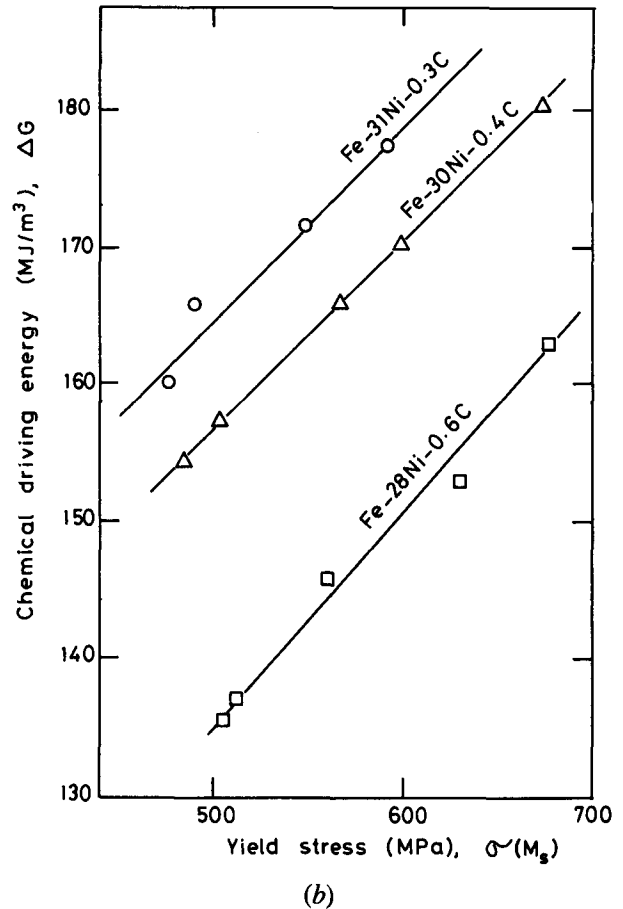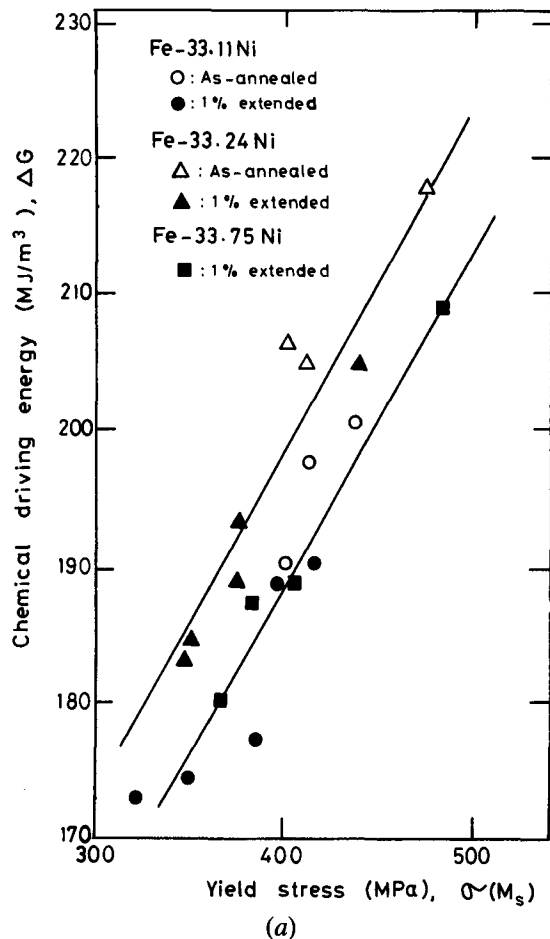
Fig. 12 — Relation between chemical driving energy and austenite yield stress at the start of the martensitic transformation: (a) for Fe-Ni alloys and (b) for Fe-Ni-C alloys.

Now let us evaluate the value of $\alpha$ for these alloys. The shape strain of the martensite can be calculated by the phenomenological theory,[31,32] the validity of which has been confirmed experimentally in many cases.[23,33] So, in the present analysis, the theoretically predicted crystallographic features of the martensitic transformation were used. The calculated shear strain $\gamma$ is 0.22 for both the Fe-Ni and Fe-Ni-C alloys. The habit plane and the shear direction of the shape strain are close to (3 15 10) and [1$\bar{3}$3], respectively, for both cases. In order to accommodate such shape strain of the martensite, two slip systems, [0$\bar{1}$1]($\bar{1}$11) and [0$\bar{1}$1](111), must be operated in the austenite. Using Eqs. [9] through [11] in Reference 24, the orientation factors $m$ of these systems were found to be 0.670 and 0.850 for the Fe-Ni alloys, and 0.695 and 0.858 for the Fe-Ni-C alloys, respectively.* The smaller value was taken to esti-

*The small difference in $m$ between the Fe-Ni and Fe-Ni-C alloys is ascribed to the difference in lattice parameter which results in slightly different habit planes and shear directions according to the phenomenological theory.

mate $\alpha$, for, by the relationship of $m\tau = \tau_c$, the other slip system, i.e., [0$\bar{1}$1](111), which has a larger value of $m$, also becomes active. According to Taylor, $M = 3.1$ for fcc polycrystals.[25,26] Thus we have $\alpha = 0.106$ and 0.102 for the Fe-Ni and Fe-Ni-C alloys, respectively. The slopes in Figures 12(a) and (b) are 0.25 and 0.15, which are to be compared with the above calculated values of $\sigma$. Consid-

ering the ambiguities involved in the estimation of the chemical driving energy at low temperatures, we can say that the agreement between the calculated and experimental values of $\alpha$ is fairly good. The reason for somewhat larger values of the experimentally determined $\alpha$ may be that $\sigma$ in Eq. [1] was taken as yield stress of austenite. Since the shear strain of the shape deformation is as large as 0.22, the resistive stress acting on the transforming martensite will be larger than the yield stress due to work hardening. This effect is more prominent in small grain size specimens, for the accommodation shear strain in the austenite is considered to increase with decreasing grain size owing to increasing ratio of the martensite plate thickness to the grain diameter. If such effect is taken into account, the slope in Figures 12(a) and (b) would become smaller. The accommodation slip is observed more extensively in the Fe-Ni alloys where a lenticular martensite is formed. This fact indicates that the work hardening effect mentioned above is more important in the Fe-Ni alloys, and it may explain a larger deviation of the observed value of $\alpha$ from the theoretical one. Thus we can conclude that the increased yield strength of austenite by grain refining is the principal factor for depressing $M_s$ in fine-grained specimens.

Now we discuss why the effect of grain size on $M_s$ is small for the alloys of which the plateau temperature, $T_p$, of the $M_s$ vs grain size curve is high. There seem to be two factors responsible for this phenomenon. One is that the temperature dependence of austenite yield stress, $\partial\sigma/\partial T$, is

decreased with increasing temperature as seen in Figure 9. As noted previously, the increase in $\sigma(M_s)$ is the sum of the increases due to grain refinement and temperature decrease. The contribution by the latter term is considerable in alloys No. 3, 5 through 7; in some cases it amounts to about $\frac{1}{3}$ of the total increase. However, in the case of a small value of $\partial\sigma/\partial T$, this latter contribution becomes small, thus reducing the work necessary for the plastic accommodation. This effect will be especially prominent for alloys having $M_s$ above room temperature, because $\partial\sigma/\partial T \approx 0$ in such a temperature range. The other factor is that the temperature dependence of the chemical driving energy, $\partial\Delta G/\partial T$, is larger in a higher temperature range as seen in Figure 11, which means that a small temperature decrease is sufficient to supply an energy to counterbalance the extra work caused by an increase in the austenite yield stress due to grain refinement. On the other hand, in a low temperature range, $\sigma$ increases very rapidly with decreasing temperature, while the chemical driving energy does not increase very much. These factors are combined to cause a prominent decrease in $M_s$ with grain refinement for the case of low $T_p$. In the present investigation it was frequently experienced that a specimen which had not been transformed above 77 K was not transformed either by immersing in liquid helium. This is also considered to be due to the factors mentioned above.

## IV. CONCLUDING REMARKS

It has been shown in the present work that the plastic accommodation in austenite is a very important step in the nucleation event. This point has not been taken into account in any nucleation models so far proposed. In order for a martensite plate to be brought into existence from a potential nucleation site, three kinds of deformation must take place except for some special cases: that is, the "lattice deformation" which generates a martensite lattice from austenite, the "lattice invariant deformation" which produces an interface with no average distortion between the two phases (*i.e.*, an invariant habit plane), and the deformation which accommodates the shape strain of the martensite plate. From the crystallographic analysis of fully grown martensite plates it has been shown in various alloys that the shape strain of the martensite plate is usually self-accommodated by forming several variants of martensite.[34-37] The self-accommodating martensite variants were also observed in the present Fe-Ni and Fe-Ni-C alloys. However, this fact does not necessarily mean that such self-accommodation occurs also in the nucleation stage. From the experimental results and the discussion presented in the preceding section, a different conclusion has been drawn that the shape strain of the nucleating martensite must be accommodated by plastic deformation in austenite, and that any factors impeding the plastic accommodation, such as the lack of dislocations, work hardening, and grain refinement, suppress the transformation.

The effect of work hardening on $M_s$ is very prominent in the case where no self-accommodation effect occurs even in a later stage of the martensite formation. One example for such case is seen in the isothermal martensitic transformation of Fe-Ni-Mn alloys. In these alloys the plastic accommodation of the martensite shape strain continues to
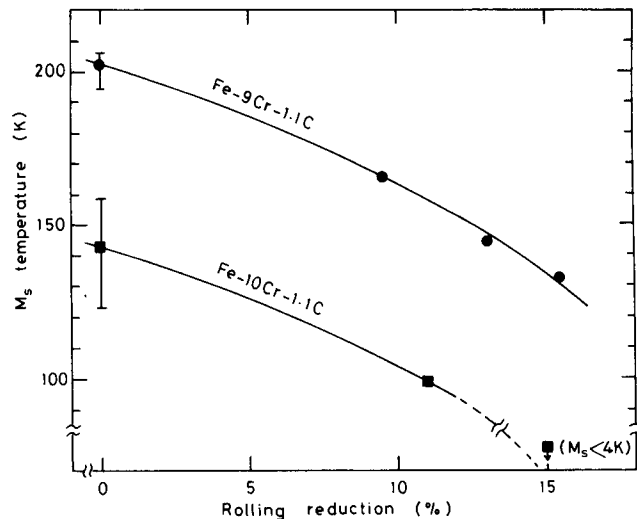


Fig. 13—Effect of rolling reduction on $M_s$ temperature of Fe-9Cr-1.1C and Fe-10Cr-1.1C. Specimens were initially austenitized at 1520 K for 1 h. The $M_s$ temperature for the as-austenitized state is an average of $M_s$'s of four measurements.

occur until the martensite plate has fully grown,[38,39] and it was found previously by the present author that the initial rate of the isothermal transformation is very much decreased with increasing amount of prestrain.[38] Another example is the athermal martensitic transformation of Fe-Cr-C alloys, in which the mode of the accommodation of the martensite shape strain is similar to that of Fe-Ni-Mn alloys.[40] Figure 13 shows the effect of prestrain on $M_s$ in Fe-9Cr-1.1C and Fe-10Cr-1.1C (alloys No. 9 and 10). The prestrain was introduced by rolling at room temperature. The $M_s$ temperature is remarkably decreased with increasing rolling reduction. For Fe-10Cr-1.1C, the effect is more drastic; a 15 pct rolling reduction depressed $M_s$ below 4 K from 145 K. In these examples, it is considered that non-prestrained specimens had already contained a sufficient number of dislocations* to initiate the plastic accommo-

---

*In these experiments specimens austenitized at high temperatures were quenched to room temperature, which inevitably causes some extent of deformation.

---

dation, and the prestraining introduced an excess number of dislocations which acts only as a barrier to moving dislocations. The above two experimental facts clearly demonstrate that the plastic accommodation of the shape strain of martensite is an indispensable condition for the martensite nucleation.

In conclusion, the results of the present work are summarized as follows:

1. Contrary to the general belief, dislocations themselves do not act as favorable nucleation sites in the martensitic transformation.
2. The existence of dislocations helps martensite nucleation only in the sense that it can serve plastic accommodation of the shape strain of martensite.
3. The introduction of too many dislocations in austenite hinders martensite nucleation due to work hardening.
4. Grain boundaries seem to be favorable nucleation sites, but all the boundaries can not serve as nucleation sites. Only those boundaries which have some special character

are qualified to be potential nuclei, although the character of such boundaries was not able to be specified in the present study.

5. A quantitative analysis supports the proposition that the factor for depressing $M_s$ in fine-grained specimens is the increased yield strength of austenite by grain refining.

## REFERENCES

1. E. S. Machlin and M. Cohen: *Trans. AIME*, 1951, vol. 191, pp. 746-54.
2. H. C. Fiedler, B. L. Averback, and M. Cohen: *Trans. ASM*, 1955, vol. 47, pp. 267-90.
3. R. E. Cech and D. Turnbull: *Trans. AIME*, 1956, vol. 206, pp. 124-32.
4. L. Kaufman and M. Cohen: *Progr. Met. Phys.*, 1958, vol. 7, pp. 165-246.
5. Y. Hosoi and Y. Kawakami: *Tetsu-to Hagané*, 1963, vol. 49, pp. 1780-87 (in Japanese).
6. G. B. Olson and M. Cohen: *Metall. Trans. A*, 1976, vol. 7A, pp. 1897-1923.
7. M. Suezawa and H. E. Cook: *Acta Metall.*, 1978, vol. 26, pp. 1205-13, *ibid.*, 1980, vol. 28, pp. 423-32.
8. J. R. C. Guimaraes and J. C. Gomes: *Acta Metall.*, 1978, vol. 26, pp. 1591-96.
9. M. R. Meyerson and S. J. Rosenberg: *Trans. ASM*, 1954, vol. 46, pp. 1225-53.
10. M. G. H. Wells and D. R. F. West: *J. Iron and Steel Inst.*, 1962, vol. 200, pp. 472-73.
11. A. S. Sastri and D. R. F. West: *J. Iron and Steel Inst.*, 1965, vol. 203, pp. 138-45.
12. O. A. Ankara, A. S. Sastri, and D. R. F. West: *J. Iron and Steel Inst.*, 1966, vol. 204, pp. 509-11.
13. A. R. Entwisle and F. A. Feeney: The Institute of Metals, Monograph and Report Series No. 33, 1969, pp. 156-61.
14. T. Maki, S. Shimooka, M. Umemoto, and I. Tamura: *Nippon Kink. Gakk.*, 1971, vol. 35, pp. 1073-82 (in Japanese).
15. T. Maki, S. Shimooka and I. Tamura: *Metall. Trans.*, 1971, vol. 2, pp. 2944-45.
16. M. Umemoto and W. S. Owen: *Metall. Trans.*, 1974, vol. 5, pp. 2041-46.
17. T. J. Nichol, G. Judd, and G. S. Ansell: *Metall. Trans. A*, 1977, vol. 8A, pp. 1877-83.
18. P. J. Brofman and G. S. Ansell: *Metall. Trans. A*, 1983, vol. 14A, pp. 1929-31.
19. E. M. Breinan and G. S. Ansell: *Metall. Trans.*, 1970, vol. 1, pp. 1513-20.
20. S. J. Donachie and G. S. Ansell: *Metall. Trans. A*, 1975, vol. 6A, pp. 1863-75.
21. R. Pradhan and G. S. Ansell: *Metall. Trans. A*, 1978, vol. 9A, pp. 793-801.
22. G. S. Ansell, P. J. Brofman, T. J. Nichol, and G. Judd: *Proc. 3rd Int. Conf. on Martensitic Transformation*, Cambridge, MA, 1979, pp. 350-55.
23. C. M. Wayman: *Introduction to the Crystallography of Martensitic Transformations*, The Macmillan Company, 1964.
24. J. P. Hirth and J. Lothe: *Theory of Dislocations*, McGraw-Hill, 1968, pp. 272-75.
25. G. I. Taylor: *J. Inst. Metals*, 1938, vol. 62, pp. 307-24.
26. A. H. Cottrell: *Dislocations and Plastic Flow in Crystals*, Oxford University Press, London, England, 1965, pp. 116-24.
27. J. P. Hirth: *Metall. Trans.*, 1972, vol. 3, pp. 3047-67.
28. E. O. Hall: *Proc. Phys. Soc. (London)*, 1951, vol. 64B, pp. 747-53.
29. N. J. Petch: *J. Iron Steel Inst.*, 1953, vol. 174, pp. 25-28; *Phil. Mag.*, 1956, vol. 1, pp. 866-73.
30. L. Kaufman and M. Cohen: *Trans. AIME*, 1956, vol. 206, pp. 1393-1401.
31. M. S. Wechsler, D. S. Lieberman, and T. A. Read: *Trans. AIME*, 1953, vol. 197, pp. 1503-15.
32. J. S. Bowles and J. K. Mackenzie: *Acta Metall.*, 1954, vol. 2, pp. 129-47, 224-34.
33. H. Warlimont and L. Delaey: *Progr. Mat. Sci.*, Pergamon Press, 1974, vol. 18.
34. J. C. Bokros and E. R. Parker: *Acta Metall.*, 1963, vol. 11, pp. 1291-1301.
35. H. Tas, L. Delaey, and A. Deruyttere: *Metall. Trans.*, 1973, vol. 4, pp. 2833-40.
36. T. Saburi, S. Nenno, S. Kato, and T. Takata: *J. Less-Common Metals*, 1976, vol. 50, pp. 223-36.
37. H. Okamoto, M. Oka, and I. Tamura: *Trans. Japan Inst. Met.*, 1978, vol. 19, pp. 674-84.
38. S. Kajiwara: *Phil. Mag.*, 1981, vol. A43, pp. 1483-1503.
39. S. Kajiwara: *Acta Metall.*, 1984, vol. 32, pp. 407-13.
40. B. P. J. Sandvik and C. M. Wayman: *Metall. Trans. A*, 1983, vol. 14A, pp. 2455-68.